First-Principles DFT Insights into the Mechanisms of CO2 Reduction to CO on Fe (100)-Ni Bimetals

Caroline Kwawu (kwawucaroline@gmail.com)
Kwame Nkrumah University of Science and Technology https://orcid.org/0000-0001-5686-1377
Albert Aniagyei
University of Health and Allied Sciences
Destiny Konadu
Kwame Nkrumah University of Science and Technology
Elliot Menkah
Kwame Nkrumah University of Science and Technology
Richard Tia
Kwame Nkrumah University of Science and Technology

Research Article

Keywords: CO2 decomposition, CO2 activation, bimetals, Iron alloys, Nickel deposited Surfaces

Posted Date: June 24th, 2021

DOI: https://doi.org/10.21203/rs.3.rs-540311/v1

First-Principles DFT Insights into the Mechanisms of CO_2 Reduction to CO on Fe (100)-Ni Bimetals

Caroline R. Kwawu,[1]* Albert Aniagyei,[2] Destiny Konadu,[1] Elliot Menkah,[1] Richard Tia [1]

[1]Department of Chemistry, Kwame Nkrumah University of Science and Technology, Kumasi, Ghana
[2]Department of Basic Sciences, University of Health and Allied Sciences, Ho, Ghana
Email: kwawucaroline@gmail.com (C.R.K)

Declarations

Funding:

CRK is grateful for funding from The World Academy of Sciences (grant 18-032 RG/CHE/AF/AC_I). CRK and RT acknowledges the UK Royal Society and Leverhulme Trust for a research grant under the Royal Society-Leverhulme Africa Postdoctoral Fellowship Award Scheme (grant LAF\R1\180013).

Conflicts of Interest: No conflicts of interest

Availability of data and material: No additional data available to be shared.

Code availability: Quantum Espresso is an opensource code available at https://www.quantum-espresso.org/

Author's contributions: Data was collected by Mr. Destiny Konadu, Manuscript was drafted by Dr. Caroline Rosemyya Kwawu and revised by Dr. Albert Aniagyei and Dr. Elliot Menkah. Research concept was developed and supervised by Dr. Richard Tia and Dr. Caroline Rosemyya Kwawu.

Abstract

Iron and nickel are known active sites in the enzyme carbon monoxide dehydrogenases (CODH) which catalyzes CO_2 to CO reversibly. The presence of nickel impurities in the earth abundant iron surface could provide a more efficient catalyst for CO_2 degradation into CO, which is a feedstock for hydrocarbon fuel production. In the present study, we have employed spin-polarized dispersion-corrected density functional theory calculations within the generalized gradient approximation to elucidate the active sites on Fe (100)-Ni bimetals. We sort to ascertain the mechanism of CO_2 dissociation to carbon monoxide on Ni deposited and alloyed surfaces at 0.25, 0.50 and 1 monolayer (ML) impurity concentrations. CO_2 and (CO + O) bind exothermically i.e., -0.87 eV and -1.51 eV respectively to the bare Fe (100) surface with a decomposition barrier of 0.53 eV. The presence of nickel generally lowers the amount of charge transferred to CO_2 moiety. Generally, the binding strengths of CO_2 were reduced on the modified surfaces and the extent of its activation was lowered. The barriers for CO_2 dissociation increased mainly upon introduction of Ni impurities which is undesired. However, the 0.5 ML deposited ($FeNi_{0.5}$(A)) surface is promising for CO_2 decomposition, providing a lower energy barrier (of 0.32 eV) than the pristine Fe (100) surface. This active 1-dimensional defective $FeNi_{0.5}$(A) surface provides a stepped surface and Ni-Ni bridge binding site for CO_2 on Fe (100). Ni-Ni bridge site on Fe (100) is more effective for both CO_2 binding or sequestration and dissociation compared to the stepped surface providing the Fe-Ni bridge binding site.

Keywords: CO_2 decomposition; CO_2 activation; bimetals; Iron alloys; Nickel deposited Surfaces

1. INTRODUCTION

The levels of carbon dioxide in the atmosphere continues to increase as a result of anthropogenic activities like combustion of fossil fuels, leading to global warming and climate change.[1] CO_2 is an abundant and cheap carbon-one source, which could be a useful feedstock in the production of transportation fuels,[2] industrial chemicals,[3] and polymers.[1] However, due to the stability and inertness of the CO_2 molecule, catalysts are required for conversion.[4, 5] Despite difficulties associated with CO_2 conversion industrially, anaerobic enzymes such as carbon monoxide dehydrogenases are known to reversibly catalyze the reduction of CO_2 to CO at ambient conditions of temperature and pressure.[6] CO_2 is said to anchor and receive electrons at the bridge site of iron and nickel in the

Fe-Ni-S cluster in carbon monoxide dehydrogenases.[7] The catalytic CO_2 decomposition into CO has become an active field of research in catalytic chemistry as CO is the feedstock in the Fischer-Tropsch process for the production of long-chain hydrocarbon liquid transportation fuels.[2, 8]

Catalytic conversion of CO_2 to valuable industrial feedstock like CO is an attempt to ease the effects of CO_2 on our environment. Although experimental studies on CO_2 reduction on single crystal surfaces show activity for CO_2 chemisorption and reduction on bare Fe and Ni, including Ni (110) and Fe (111), [9] the energetics and mechanisms of CO_2 transformation to viable products like CO, methane, formic acid etc. on these bare metal surfaces were not well understood. The extent of CO_2 activation and dissociation on iron and nickel surfaces have been shown to be face specific experimentally.[10–14]

This was later supported by other density functional theory (DFT) calculations whereby on iron the barrier to CO_2 dissociation on the low Miller index surfaces were of the trend Fe (100) ~ (111) < (110).[15] Several computational studies have also been carried out to investigate the interactions of CO_2 with Ni, mostly employing the spin-polarized density functional theory-generalized gradient approximation (DFT-GGA) to understand the energetics on their various topologies. [16–24] CO_2 is reported to bind more strongly on iron than nickel while its decomposed species bind stronger to nickel than iron. Kinetically decomposition is observed to be favored on iron than nickel. [21]

Iron and nickel are known active sites in the enzyme carbon monoxide dehydrogenases (CODH) and the presence of nickel impurity in earth-abundant iron could provide more active materials for CO_2 decomposition to CO. CO_2 interactions with bare and 1 ML deposited surfaces of the low Miller index surfaces of iron have been investigated previously,[15] where nickel is seen to alter the ease of CO_2 dissociation. However, to the best of our knowledge, no theoretical studies have been carried out on alloys of iron and nickel and the concentration effect of nickel deposition on the activity of the iron surface has also not been explored. In this present study, we have employed dispersion-corrected spin-polarized-density functional theory calculations within the generalized gradient approximation (DFT-D2-GGA) to elucidate the mechanism of CO_2 reduction into carbon monoxide on the pristine Fe (100) facet, its nickel alloys and nickel deposited surfaces at varying concentrations of 0.25 ML, 0.5 ML and 1 ML.

2. COMPUTATIONAL DETAILS

All calculations were carried out with the spin-polarized density functional theory method as implemented in the Quantum ESPRESSO package.[25] The generalized gradient approximation (GGA), with the Perdew, Burke, Ernzerhof (PBE) exchange-correlation functional[26] was used in all simulations. The surface was described by a slab model, where periodic boundary conditions were applied to the central super-cell so that it is reproduced periodically throughout space. XcrysDen [27] software was employed for the visualization of structures and electron densities. The Fermi-surface effects were treated by the smearing technique of Fermi-Dirac, using a smearing parameter of 0.03 Ry. The energy threshold defining self-consistency of the electron density was set to 10^{-6} eV.

Iron (100) surface was cleaved with the METADISE code [28] and a *p*(2x2) super-cell was employed for all calculations as the binding energy of CO_2 does not change significantly with increasing super-cell. The slab was built to a thickness of three, made up of six atomic layers. A vacuum of 20 Å was introduced to the surface to prevent interactions between surfaces along the z-axis. The top three layers of the slab was relaxed in all calculations, which has been reported previously to be the converged structure of iron (100).[29] All gaseous adsorbates were optimized in a cubic box of size 20 Å and allowed to relax in all calculations. Neighboring adsorbates in laterally repeating units of the slabs were more than 5 Å apart.

Using convergence tests, the kinetic energy cutoff of the plane wave basis set was set to 40 Ry and 320 Ry for the charge density cut-off. The Monkhorst-pack K-points grid of (7 x 7 x 7), (5 x 5 x 1) and (1 x 1 x 1) were used for bulk, surfaces and adsorbates respectively. The Climbing Image Nudged Elastic Band (CI-NEB) method was used to determine the energy barriers for dissociation. Vibrational modes were calculated whereby a single imaginary frequency was indicative of a transition state. Lowdin charge analysis was employed for charge density characterizations upon adsorption of CO_2.

3. RESULTS AND DISCUSSION

3.1 CO_2 adsorption on Pure and Bimetallic Surfaces

The computation parameters were first validated by calculating the bulk properties of iron. The unit cell of iron crystalizes in the body-centered cubic (BCC) form and our spin-polarized DFT-D2 calculations were able to reproduce the electronic properties of bulk iron.[15, 30]

We considered six different bi-metallic surfaces, i.e., nickel adsorption and absorption as a point defect (P), 1-dimensional defect (1D) and 2-dimensional defect (2D). Hence nickel ad-atom deposition at 3 concentrations i.e., 0.25 ML ($FeNi_{0.25}$(A)), 0.5 ML ($FeNi_{0.5}$(A)) and 1 ML ($FeNi_1$(A)), and nickel alloying at 3 concentrations i.e., 0.25ML ($FeNi_{0.25}$(B)), 0.5ML ($FeNi_{0.5}$(B)) and 1-ML ($FeNi_1$(B)) (see **Figure 1**). The energetics of bi-metallic surface formation was determined using the defect formation energies below in equation (1);

$$Edef = Eproducts - Ereactants \quad (1)$$

Equation (1) represents formation energy for the deposition or adding on of ad-atoms and Equation (2) represents formation energy for the doping or replacement of host atoms.

$$Edef = \frac{Edeposited - (Eslab + nENi)}{n} \quad (2)$$

$$Edef = \frac{(Edoped + nEFe) - (Eslab + nENi)}{n} \quad (3)$$

Where E_{Fe} is energy of single iron atom, E_{Ni} is energy of single nickel atom, n is the number of dopants and E_{slab} is energy of the perfect Fe (100) surface.

Table 1: The binding strength of CO_2 (E_{ads}), charge gained by CO_2 (q), the extent of CO_2 activation (C-O $_{Avg}$) and the Fermi energy (E_f) of Ni modified Fe (100) surfaces

Surface	E_{def}/ eV	E_{ads}/ eV	q/ e^-	C-O $_{(1)}$/ Å	C-O $_{(2)}$/ Å	C-O $_{Avg}$/ Å	E_f/ eV
i. Bare Fe	-	-0.87	0.08	1.35	1.36	1.36	3.07

a. $FeNi_{0.25}$(A)	-8.47	-0.33	0.04	1.25	1.25	1.25	2.04
b. $FeNi_{0.5}$(A)	-4.88	-0.47	0.04	1.25	1.25	1.25	2.06
c. $FeNi_1$(A)	-5.29	-0.19	0.06	1.30	1.32	1.31	0.90
d. $FeNi_{0.25}$(B)	4.02	-0.92	0.08	1.34	1.35	1.35	2.91
e. $FeNi_{0.5}$(B)	0.53	-0.96	0.08	1.34	1.35	1.35	2.86
f. $FeNi_1$(B)	-0.70	-0.84	0.08	1.34	1.35	1.35	2.73

As seen in **Table 1**, deposition is generally favored thermodynamically over alloying, nickel prefers to be segregated on iron than alloy at all concentrations of 0.25 to 1 ML. The high instability of the doped surfaces relative the deposited surfaces show that thermodynamically at 0.25 ML, 0.5 ML and 1 ML concentrations, nickel will be segregated on the surfaces than diffuse to form alloys with the Fe (100) surface. The stability of the Fe-Ni alloys increases with nickel concentration and iron nickel mixing could improve with higher impurity concentrations. The defect formation energies show a stability trend of $FeNi_{0.25}$(B) < $FeNi_{0.5}$(B) < $FeNi_1$(B) < $FeNi_1$(A) < $FeNi_{0.5}$(A) < $FeNi_{0.25}$(A). The high stability of $FeNi_{0.25}$(A) over $FeNi_1$(A) shows that the nickel once on the surface of iron prefers to isolate from neighboring nickel atoms than to coagulate on the surface of iron.

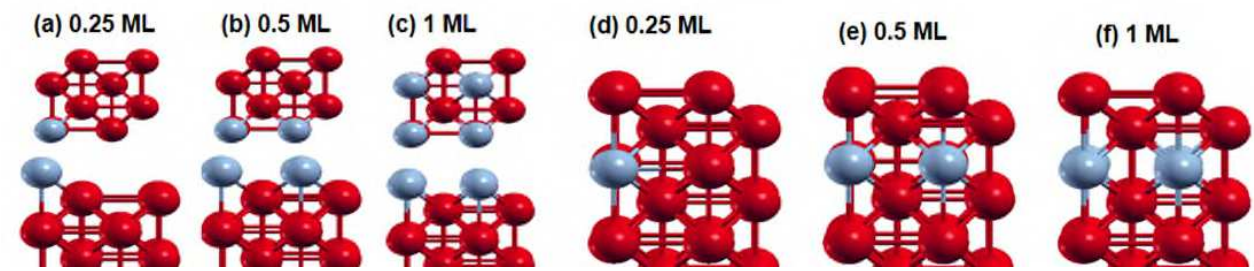

Figure 1: Defect formation energies of nickel with iron surfaces, (a) deposition at 0.25 ML, (b) deposition at 0.5 ML, (c) deposition at 1 ML, (d) doping at 0.25 ML, (e) doping at 0.5 ML and (f) doping at 1 ML

Carbon dioxide adsorption was then studied on the pure and defective surfaces (see **Figure 2**) and the binding energies of CO_2 on the various surfaces were calculated as follows;

$$Eads = E(slab + CO2) - (Eslab + ECO2) \quad (4)$$

Where $E_{(slab+CO2)}$ is the energy of the adsorbed system, E_{slab} and E_{CO2} are the energies of the isolated surface and gaseous carbon dioxide respectively.

The preferred CO_2 adsorption site on the clean Fe (100) surface has been reported to be the hollow site in the C_{2V} adsorption mode. [15] At the active site i.e., at the hollow site and in the C_{2V} preferred CO_2 adsorption state, we investigated the effect of doping on CO_2 binding.

As shown in **Figure 3**, CO_2 binding to bare Fe (100) is exothermic with adsorption energy of -0.87 eV. This is very consistent with earlier observations of -0.9 eV, [15] -0.92 eV,[31] -0.7 eV.[19] Introduction of nickel into the bulk of iron (structure d) at point defect of 0.25 ML, increases the binding strength of CO_2 to -0.92 eV. CO_2 coordinates to four iron atoms at the hollow site. Increasing the nickel concentration to 1D defect (structure e) increases the iron-CO_2 interactions at the hollow site to -0.96 eV. Whiles at 2D defect (structure f), the iron-CO_2 interaction at the hollow site is decreased to -0.84 eV, this is less than the binding on bare Fe (100). Comparing the electronegativity of nickel and iron, nickel is more electron withdrawing and increasing its concentration in the bulk of iron, lowers the electron density available at the surface for transfer into the CO_2 moiety. The nickel electron withdrawing effect is felt at the surface with increasing concentration of nickel. Also increasing the concentration of nickel dopant at the sub-surface site introduces appreciable Ni properties at the surface, as bare Ni is known to bind CO_2 more weakly. [32]

In Ni adsorption situations as shown in Figure 3a and 3b, stepped surfaces are provided that provide lower surface η-CO_2 coordination and lower binding energies due to the presence of nickel on surfaces compared to the alloyed surfaces in Figure 3d, 3e and 3f. As seen for the nickel single ad-atom at 0.25 ML deposition, the binding takes place at the bridge of iron and nickel, and the strength of binding is weakened to -0.33 eV compared to bare iron. Increasing nickel concentration at the surface decreases the binding strength of CO_2 further to -0.19 eV for ($FeNi_1$(B)) (c).

Ni generally weakens CO_2 binding strength except in cases where the Ni effect is less felt on the surface. These results show that decreasing CO_2 surface coordination by the introduction of adatoms and higher electronegative atom effects like nickel on the surface weakens CO_2 binding.

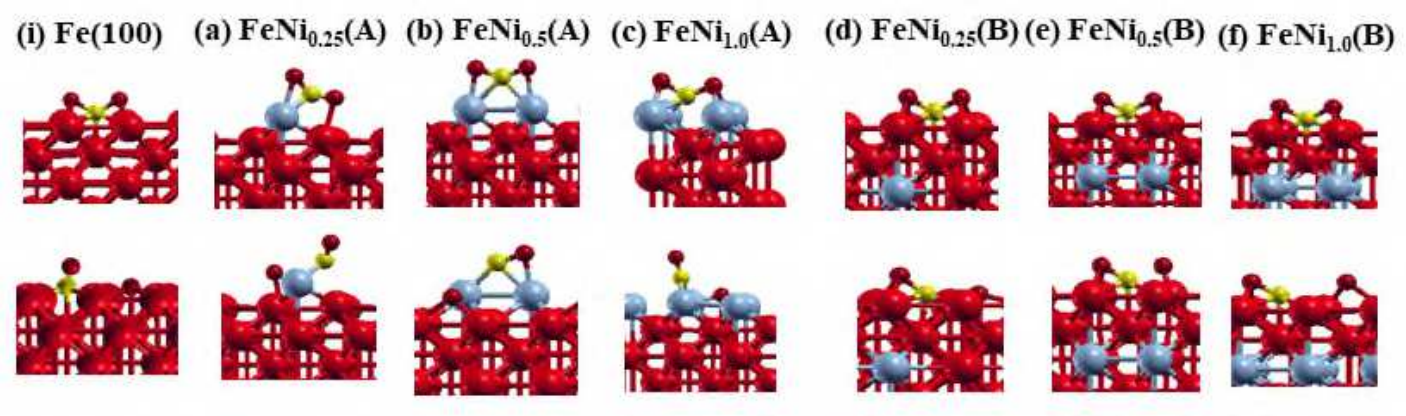

Figure 2: CO_2 adsorption on the bare, deposited and doped Fe (100)-Ni surfaces

The net amount of charge gained by CO_2 molecule from the surface and the extent of CO_2 activation on the surfaces has also been characterized and reported in **Table 1**. To understand the factors controlling the CO_2 binding strength and the extent of CO_2 activation various plots were carried out (see **Figure 3**). A plot of CO_2 degree of activation and the amount of charge gained by CO_2 (**Figure 3d**), shows that the more the charge gained by the molecule the more activated the molecule. This is consistent with earlier studies.[23] A regression factor of 0.99 was obtained. A plot of the surface Fermi energy and the amount of charge gained by the CO_2 moiety shows there is no correlation with a regression factor of 0.02. Although the Fermi energy and the charge loss by the surface do not correlate, there is a correlation between the surface Fermi energy and the binding strength of CO_2. With a regression factor of 0.86 (see **Figure 3c**). Hence Fermi energy does not influence charge transfer and CO_2 degree of activation but influences the binding strength. Generally, Ni impurities reduce the Fermi energy and binding strength of CO_2 to the surfaces. There is however, weak correlation of 0.60 and 0.67 between the binding energy and the variables of CO_2 activation (plot b) and charge gained (plot a) respectively.

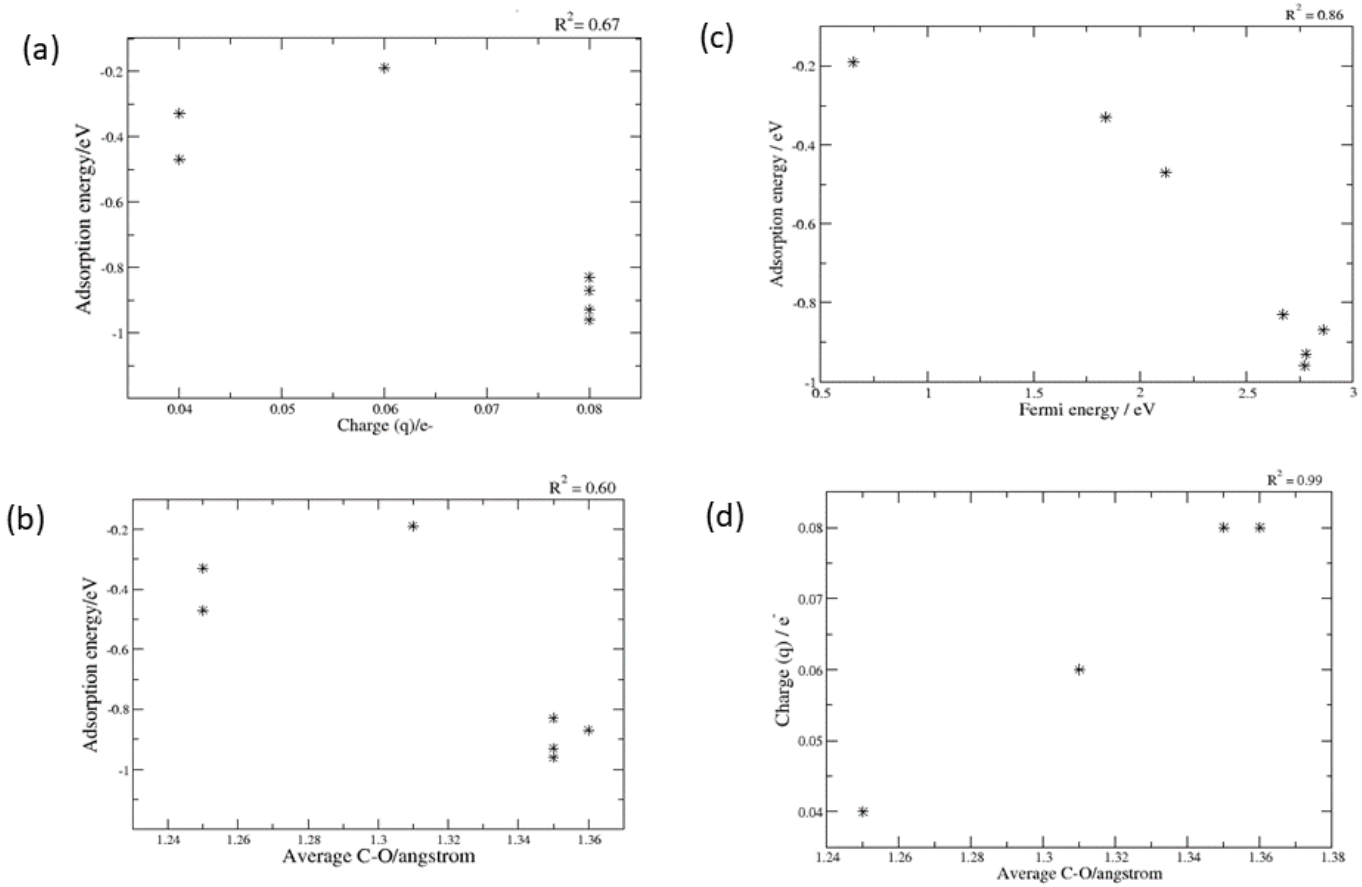

Figure 3: Plot of (a) CO_2 binding energy against charge gained by CO_2 molecule (b) CO_2 binding energy against CO_2 extent of activation, (c) CO_2 binding energy against Fermi energy of surface, (d) Charge gained by CO_2 molecule against CO_2 extent of activation

3.2 CO_2 Dissociation on Pure and Bimetallic Surfaces

The reaction energies for CO_2 dissociation (E_{dis}) and the barriers for dissociation (E_a) were calculated with equation (2) and (3) respectively;

$$E_{dis} = E_{products} - (E_{slab} + E_{CO2}) \qquad (2)$$

Where $E_{products}$ is the energy of the adsorbed dissociated system, E_{slab} is the energy of isolated slab and E_{CO2} is the energy of isolated carbon dioxide molecule.

$$E_a = E_{TS} - E_{IS} \quad (2)$$

Where E_{TS} is energy of the transition state and E_{IS} is the energy of the intermediate state i.e., adsorbed CO_2.

To reduce surface interaction between adsorbed molecules, the decomposed species CO and O were optimized individually on the surfaces as well to determine the binding energies in **Table 2**. As reported in **Table 2**, the binding energy of decomposed CO_2 (E_{dis}), is generally favorable thermodynamically relative to the binding energy of CO_2 (E_{ads}). The thermodynamics of the dissociation steps were also calculated relative to the activated CO_2 moiety ($Step_{dis}$) and was found to be a thermodynamically favored step on all surfaces. The reaction barriers for the dissociation steps were then computed for the reactions on the various surfaces. The energy profile diagram showing the energy transitions along the reaction coordinates are shown in **Figure 4**.

Table 2: Energies for the adsorption and dissociation reactions as well as energy barriers for each dissociation step

Surface	ΔE_{ads}/ eV	ΔE_{dis}/ eV	$Step_{dis}$/ eV	E_a/ eV
i. Bare Fe	-0.87	-1.51	-0.64	0.53
a. $FeNi_{0.25}$(A)	-0.33	-0.83	-0.50	1.97
b. $FeNi_{0.5}$(A)	-0.47	-0.79	-0.32	0.32
c. $FeNi_1$(A)	-0.19	-0.52	-0.33	4.16
d. $FeNi_{0.25}$(B)	-0.92	-2.14	-1.22	0.73
e. $FeNi_{0.5}$(B)	-0.96	-2.14	-1.18	1.32
f. $FeNi_1$(B)	-0.84	-1.91	-1.07	1.27

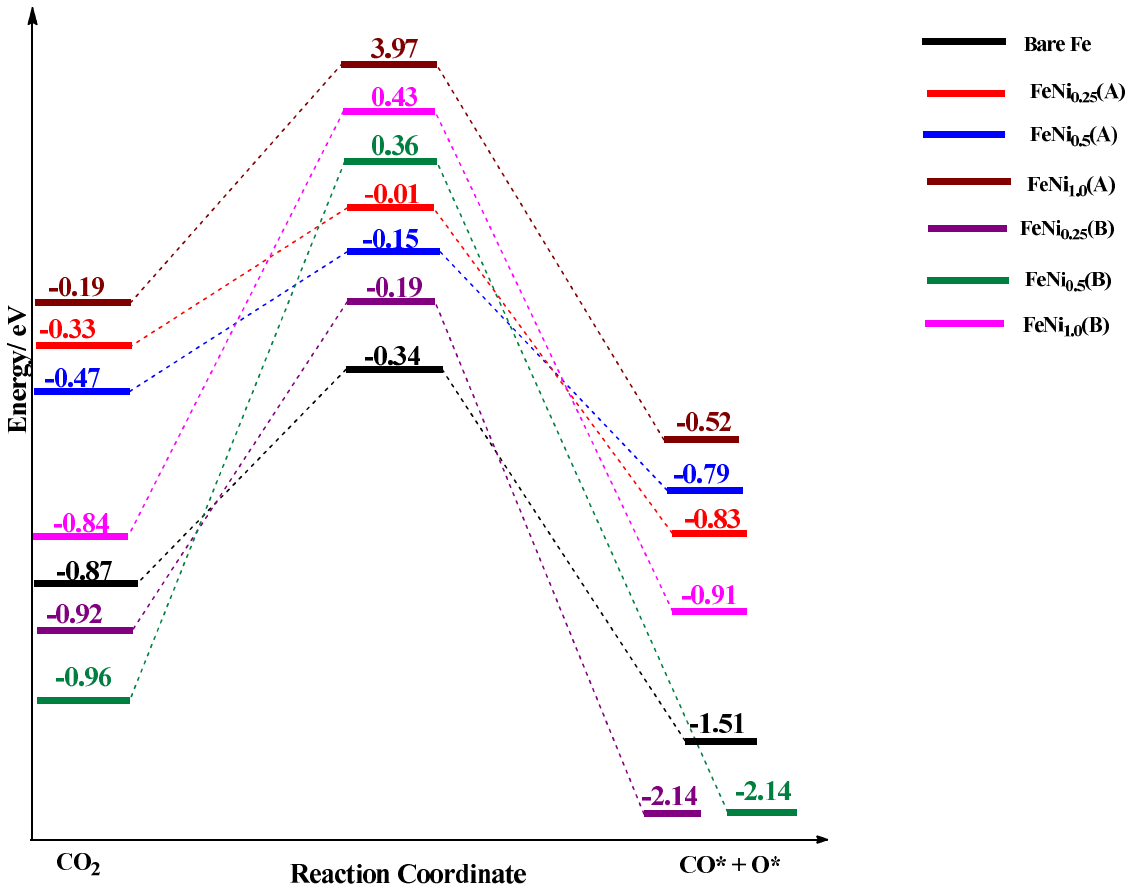

Figure 4: Reaction energy profile diagram for CO_2 dissociation on Fe (100) surfaces i.e., pure (Bare Fe), Ni deposited ($FeNi_{0.25}$(A), $FeNi_{0.5}$(A), $FeNi_1$(A)) and Ni doped ($FeNi_{0.25}$(B), $FeNi_{0.5}$(B), $FeNi_1$(B)) iron

On bare Fe (100), a dissociation barrier of 0.53 eV was found. Earlier studies reported 0.22 eV[19] and 0.8 eV.[33] Comparing the energy barriers for the CO_2 dissociation step (E_a in **Table 2**), generally nickel impedes CO_2 dissociation as higher barriers are encountered on the modified surfaces compared to the pure Fe (100) surface. Ease of dissociation is in the order $FeNi_{0.5}$(A) > Fe (100) > $FeNi_{0.25}$(B) > $FeNi_1$(B) > $FeNi_{0.5}$(B) > $FeNi_{0.25}$(A) > $FeNi_1$(A). Monolayer deposited (1 ML) $FeNi_1$(A) surface seems to be the most challenged surface for CO_2 dissociation kinetically, with a barrier of 4.16 eV. This is expected as it is the surface with most nickel atoms and nickel effect on the surface. Here the nickel behaviour is predominating, as nickel surface provide higher decomposition barriers relative to iron.[32] The $FeNi_{0.5}$(A) (1D defect) is promising for CO_2 dissociation kinetically where CO_2 is coordinated at a Ni-Ni bridge site. Although $FeNi_{0.5}$(A) is the least stable of the deposited surfaces, its formation is

thermodynamically favoured and it is also the deposited surface that binds CO_2 the most and is most suitable for CO_2 sequestration.

4. CONCLUSION

The effect of Ni alloying and deposition on the ease of CO_2 direct dissociation has been studied using the DFT method. Nickel prefers to be segregated on iron than alloy at concentration of 0.25 ML up to 1 ML as alloying is seen to be unstable. The stabilities of the modified surfaces were of the order, $FeNi_{0.25}(B) < FeNi_{0.5}(B) < FeNi_1(B) < FeNi_1(A) < FeNi_{0.5}(A) < FeNi_{0.25}(A)$. CO_2 binds exothermically to bare Fe (100) surface (E_{ads} = -0.87eV). Ni at the bulk site improves the binding of CO_2 and its applicability for CO_2 sequestration except at 1 ML doping, where the effect of bulk Ni is stronger on the surface. These results show that introduction of high amount of nickel in the bulk of iron weakens CO_2 binding. The Fermi energy of the modified surfaces have a strong correlation to the CO_2 binding strength. Thermodynamically, dissociation is favoured on all surfaces probed. Kinetically, CO_2 dissociation is most favoured on the $FeNi_{0.5}(A)$ surface, which is stepped and allows CO_2 to coordinate to two surface Ni atoms. Generally, the barriers for CO_2 dissociation are heightened compared to bare Fe (100), especially on the monolayer deposited (1 ML) $FeNi_1(A)$ surface. Ni deposition on Fe at 0.5 ML coverage could offer the most viable nickel-modified iron surface for CO_2 reduction and would provide a more reactive surface for CO_2 hydrogen unassisted splitting into CO (a feedstock essential for the Fischer-Tropsch process).

5. ACKNOWLEDGEMENT

C.R.K. is grateful for funding from The World Academy of Sciences (grant 18-032RG/CHE/AF/AC_I). C.R.K. and R.T acknowledge the UK Royal Society and Leverhulme Trust for a research grant under the Royal Society-Leverhulme Africa Postdoctoral Fellowship Award Scheme (grant LAF\R1\180013). The authors acknowledge the Centre for High-Performance Computing (CHPC), South Africa, for additional computing resources.

REFERENCES

1. Sakakura T, Choi J-C, Yasuda H (2007) Transformation of carbon dioxide. Chem Rev 107:2365–87. https://doi.org/10.1021/cr068357u

2. Jiang Z, Xiao T, Kuznetsov VL, Edwards PP (2010) Turning carbon dioxide into fuel. Philos Trans A Math Phys Eng Sci 368:3343–64. https://doi.org/10.1098/rsta.2010.0119

3. Arakawa H, Aresta M, Armor JN, et al (2001) Catalysis research of relevance to carbon management: progress, challenges, and opportunities. Chem Rev 101:953–96

4. Solymosi F (1991) The bonding, structure and reactions of CO2 adsorbed on clean and promoted metal surfaces. J. Mol. Catal. 65:337–358

5. Freund H-J, Roberts MW (1996) Surface chemistry of carbon dioxide. Surf. Sci. Rep. 25:225–273

6. Wächtershäuser G (1992) Groundworks for an evolutionary biochemistry: the iron-sulphur world. Prog Biophys Mol Biol 58:85–201. https://doi.org/10.1016/0079-6107(92)90022-X

7. Jeoung J-H, Dobbek H (2007) Carbon dioxide activation at the Ni,Fe-cluster of anaerobic carbon monoxide dehydrogenase. Science 318:1461–4. https://doi.org/10.1126/science.1148481

8. Schulz H (1999) Short history and present trends of Fischer – Tropsch synthesis. 186:3–12

9. Freund H-J, Behner H, Bartos B, et al (1987) CO2 adsorption and reaction on Fe(111): An angle resolved photoemission (ARUPS) study. Surf Sci 180:550–564. https://doi.org/10.1016/0039-6028(87)90225-1

10. Bauer R (1987) Summary Abstract: Face specificity of CO2 adsorption on iron surfaces. J Vac Sci Technol A Vacuum, Surfaces, Film 5:1110. https://doi.org/10.1116/1.574810

11. Behner H, Spiess W, Wedler G, Borgmann D (1986) Interaction of carbon dioxide with Fe(110), stepped Fe(100) and Fe(111). Surf Sci 175:276–286. https://doi.org/10.1016/0039-6028(86)90236-0

12. Yoshida K, Somorjai GA (1978) The chemisorption of CO, CO2, C2H2, C2H4, H2 and NH3 on the clean Fe(100) and (111) crystal surfaces. Surf Sci 75:46–60. https://doi.org/10.1016/0039-6028(78)90051-1

13. Hess G, Froitzheim H, Baumgartner C (1995) The adsorption and catalytic decomposition of CO2 on Fe(111) surfaces studied with high resolution EELS. Surf Sci 331–333:138–143. https://doi.org/10.1016/0039-6028(95)00177-8

14. Nassir MH (1993) Sequential carbon oxygen bond cleavage in chemisorption of CO2 on Fe(100). J Vac Sci Technol A Vacuum, Surfaces, Film 11:2104. https://doi.org/10.1116/1.578376

15. Kwawu CR, Tia R, Adei E, et al (2017) CO2 activation and dissociation on the low miller index surfaces of pure and Ni-coated iron metal: A DFT study. Phys Chem Chem Phys 19:19478–19486. https://doi.org/10.1039/c7cp03466k

16. Au C, Chen M (1997) A density functional study of CO 2 adsorption on the (100) face of Cu (9, 4, 1) cluster model. Chem Phys Lett 4:

17. de la Peña O'Shea V a., González S, Illas F, Fierro JLG (2008) Evidence for spontaneous CO2 activation on cobalt surfaces. Chem Phys Lett 454:262–268. https://doi.org/10.1016/j.cplett.2008.02.004

18. Dri C, Peronio A, Vesselli E, et al (2010) Imaging and characterization of activated CO_{2} species on Ni(110). Phys Rev B 82:165403. https://doi.org/10.1103/PhysRevB.82.165403

19. Glezakou V-A, Dang LX, McGrail BP (2009) Spontaneous Activation of CO 2 and Possible Corrosion Pathways on the Low-Index Iron Surface Fe(100). J Phys Chem C 113:3691–3696. https://doi.org/10.1021/jp808296c

20. Li H-J, Ho J-J (2010) Density Functional Calculations on the Hydrogenation of Carbon Dioxide on Fe(111) and W(111) Surfaces. J Phys Chem C 114:1194–1200. https://doi.org/10.1021/jp909428r

21. Liu C, Cundari TR, Wilson AK (2012) CO 2 Reduction on Transition Metal (Fe, Co, Ni, and Cu) Surfaces: In Comparison with Homogeneous Catalysis

22. Wang G-C, Jiang L, Morikawa Y, et al (2004) Cluster and periodic DFT calculations of adsorption and activation of CO2 on the Cu(hkl) surfaces. Surf Sci 570:205–217. https://doi.org/10.1016/j.susc.2004.08.001

23. Wang S-G, Liao X-Y, Cao D-B, et al (2007) Factors Controlling the Interaction of CO2 with Transition Metal Surfaces. J Phys Chem C 111:16934–16940. https://doi.org/10.1021/jp074570y

24. Wang S-G, Cao D-B, Li Y-W, et al (2005) Chemisorption of CO2 on nickel surfaces. J Phys Chem B 109:18956–63. https://doi.org/10.1021/jp052355g

25. Giannozzi P, Baroni S, Bonini N, et al (2009) QUANTUM ESPRESSO: a Modular and Open-source Software Project for Quantum Simulations of Materials. J Phys Condens Matter 21:395502. https://doi.org/10.1088/0953-8984/21/39/395502

26. Perdew JP, Burke K, Ernzerhof M (1996) Generalized Gradient Approximation Made Simple. Phys Rev Lett 77:3865–3868. https://doi.org/10.1103/PhysRevLett.77.3865

27. Kokalj A (1999) XCrySDen-A New Program for Displaying Crystalline Structures and Electron Densities. J Mol Graph Model 17:176–179. https://doi.org/10.1016/S1093-3263(99)00028-5

28. Watson GW, Kelsey ET, de Leeuw NH, et al (1996) Atomistic simulation of dislocations, surfaces and interfaces in MgO. J. Chem. Soc. Faraday Trans. 92:433

29. Kwawu CR, Tia R, Adei E, et al (2017) Applied Surface Science Effect of nickel monolayer deposition on the structural and electronic properties of the low miller indices of (bcc) iron : A DFT study. Appl Surf Sci 400:293–303. https://doi.org/10.1016/j.apsusc.2016.12.187

30. Kwawu CR, Tia R, Adei E, et al (2017) Effect of Nickel Monolayer Deposition on the Structural and Electronic Properties of the Low Miller Indices of (bcc) Iron: A DFT Study. Appl Surf Sci 400:293–303. https://doi.org/10.1016/j.apsusc.2016.12.187

31. Wang H, Nie X, Chen Y, et al (2018) Facet effect on CO2 adsorption, dissociation and hydrogenation over Fe catalysts: Insight from DFT. J CO2 Util. https://doi.org/10.1016/j.jcou.2018.05.003

32. Liu C, Cundari T, Wilson A (2012) CO2 reduction on transition metal (Fe, Co, Ni, and Cu) surfaces: In comparison with homogeneous catalysis. J Phys Chem … 116 (9):5681–5688

33. Nie X, Meng L, Wang H, et al (2018) DFT insight into the effect of potassium on the adsorption, activation and dissociation of CO2 over Fe-based catalysts. Phys Chem Chem Phys. https://doi.org/10.1039/c8cp02218f